nature genetics

Stochastic switching as a survival strategy in fluctuating environments

Murat Acar[1,2], Jerome T Mettetal[1,2] & Alexander van Oudenaarden[1]

A classic problem in population and evolutionary biology is to understand how a population optimizes its fitness in fluctuating environments[1–4]. A population might enhance its fitness by allowing individual cells to stochastically transition among multiple phenotypes, thus ensuring that some cells are always prepared for an unforeseen environmental fluctuation. Here we experimentally explore how switching affects population growth by using the galactose utilization network of *Saccharomyces cerevisiae*. We engineered a strain that randomly transitions between two phenotypes as a result of stochastic gene expression[5–9]. Each phenotype was designed to confer a growth advantage over the other phenotype in a certain environment. When we compared the growth of two populations with different switching rates, we found that fast-switching populations outgrow slow switchers when the environment fluctuates rapidly, whereas slow-switching phenotypes outgrow fast switchers when the environment changes rarely. These results suggest that cells may tune inter-phenotype switching rates to the frequency of environmental changes.

Unlike controlled laboratory environments, cells in the wild have to face and surmount the challenges raised by random fluctuations in extracellular conditions, including fluctuations in temperature, pH, and concentrations of nutrients and toxins. Early theoretical work on this topic often focused on understanding the connection between environmental fluctuations and genetic diversity[1–4]. However, recent studies demonstrating the importance of phenotypic heterogeneity in genetically identical cells have renewed an interest in studying this problem from the perspective of an isogenic population that is able to express multiple distinct phenotypes[10–17]. Without the need to sense the environment, cells could 'blindly' anticipate and survive environmental changes by randomly switching among multiple phenotypes, each fit to a particular environment. Here we focus on a system with two environments and two phenotypic states (**Fig. 1a**). If the stochastic switching between the two phenotypic states is much faster than the switching between the two environmental states, a high level of phenotypic diversity is expected (**Fig. 1b**, left panel). However, if the phenotypic switching rate is much slower than the environmental switching rate, the population is expected to be more homogenous at any given point in time (**Fig. 1b**, right panel). Which of these two strategies is more beneficial for the population is not a priori obvious.

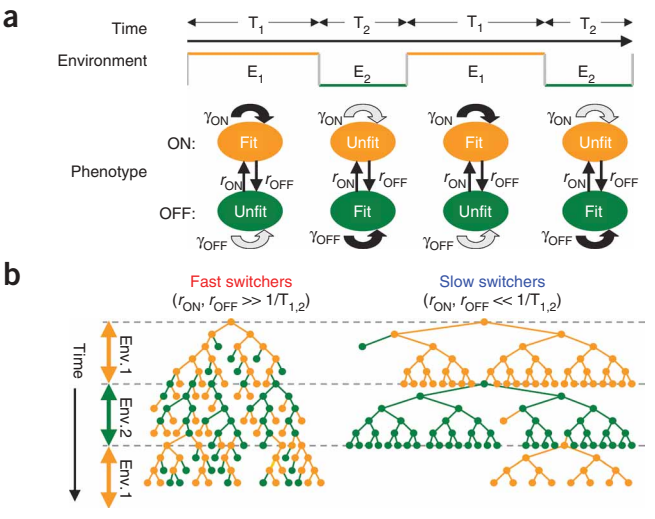

Figure 1 Stochastic switching in changing environments. (**a**) Two states (phenotypes) exist for each cell, ON (orange) and OFF (green). Cells randomly switch between the two states with frequencies r_{ON} and r_{OFF}. The first environment (E_1) has no uracil, whereas the second (E_2) has both 5-FOA and uracil. A cell is either fit or unfit to its environment depending on its specific phenotype. For example, in E_1, on-state cells are fit and have a growth rate of γ_{ON}, but the unfit off-state cells proliferate with a smaller growth rate, γ_{OFF}. (**b**) Cellular lineage for fast and slow switchers. Single cells with different switching frequencies (fast and slow) grow in alternating environments. Orange and green colors represent the first and second environments, respectively. Color change in the cellular lineage diagram corresponds to the change in phenotypic expression for a particular cell. If a cell is in the unfit state after a switching event, it ceases to proliferate. In the case of slow switchers, reduced cell-to-cell variability in each environment is depicted by a more dominant use of a single color.

[1]Department of Physics, Massachusetts Institute of Technology, Cambridge, Massachusetts 02139, USA. [2]These authors contributed equally to this work. Correspondence should be addressed to A.v.O. (avano@mit.edu).

Received 12 July 2007; accepted 14 February 2008; published online 23 March 2008; doi:10.1038/ng.110

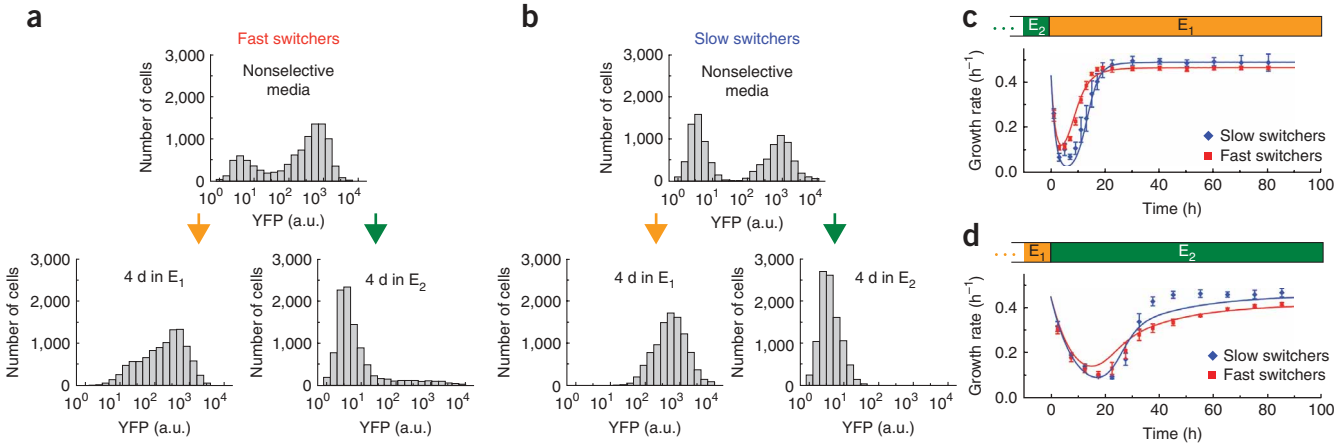

Figure 2 Environmental effects on phenotypic distribution and growth rates. (**a**) Fast-switching cells grown in nonselective media show a bimodal distribution. When cells are grown in either E_1 or E_2, the interaction of the *URA*3 gene with the environment causes ON cells to proliferate in E_1 and OFF cells to proliferate in E_2. (**b**) Similar selection is observed for slow-switching cells; however, fewer unfit cells are observed compared to the fast switchers. (**c**) Growth rates corresponding to cells prepared in an E_2 history and transferred to E_1 at $t = 0$ show a transition period and a steady-state region. Fast-switching cells (red line) recover from the effect of environment change faster than slow-switching cells (blue line) but have a lower steady-state growth rate. (**d**) Growth rates for cells prepared in an E_1 history and transferred to E_2 at $t = 0$ for fast switchers (red line) and slow switchers (blue line). Solid lines are generated by the model.

To experimentally explore how switching rates affect the population growth rate in fluctuating environments, we implemented the switching system depicted in **Figure 1a** *in vivo*. Bistable gene networks provide promising experimental systems in which to implement discrete phenotypic states, and the stochastic nature of gene expression drives rare transitions between these states[18,19]. Recently, several synthetic[20–23] and naturally occurring networks[24,25] have been shown to be bistable. We selected the bistable galactose utilization pathway of the budding yeast *S. cerevisiae*[24,26], because the switching rates between the two phenotypic states can be tuned experimentally[24]. For certain extracellular galactose concentrations, most cells in an isogenic population show either a basal pathway activity (OFF) or an activity upregulated approximately 100-fold (ON). This wild-type network was further engineered to have externally tunable stochastic transition rates, r_{ON} and r_{OFF}, between the two phenotypic expression states[24], which allowed us to define both fast ($r_{ON} \sim 0.047$, $r_{OFF} \sim 0.035$ hr^{-1}) and slow ($r_{ON} \sim 0.004$, $r_{OFF} \sim 0.007$ hr^{-1}) switching populations (**Supplementary Fig. 1** online). The activity of the pathway was read out at the single-cell level using yellow fluorescent protein (YFP) under the control of the *GAL1* promoter. To provide the two phenotypic states with two distinct growth rates, we placed the endogenous *URA3* expression, necessary for uracil biosynthesis, under the sole control of the *GAL1* promoter (**Supplementary Fig. 2** online). The two environments (E_1 and E_2) affect the growth rates of the two phenotypes in an antagonistic manner. Environment E_1 lacks uracil and therefore favors the growth of ON cells to the disadvantage of the OFF cells. In contrast, E_2 contains both uracil and the small molecule 5-fluoroorotic acid (5-FOA), which is converted into the toxic intermediate 5-fluorouracil in the presence of Ura3 protein, conferring a growth advantage to OFF cells[27]. Therefore, this experimental system provided us with a quantitative control over both the inter-phenotype switching rates and the growth rates of both phenotypes in the two different environments.

Figure 2a and **b** illustrate this antagonistic selection. In the absence of any selection, both OFF and ON cells grew at very similar rates (**Supplementary Fig. 3** online). For both the fast and slow switchers, we observed steady-state bimodal distributions of network activity (**Fig. 2a**,**b**, top panels). On the other hand, when we grew cells for 4 d in environment E_1 or E_2, the population enriched in ON or OFF cells, respectively (**Fig. 2a**,**b**, bottom panels). The fast switchers showed a more diverse distribution of expression values compared to the slow switchers, verifying our initial expectation depicted in **Figure 1b**. Next, we explored how this difference in diversity between fast and slow switchers affected the growth rate of the population. To measure growth rates over long periods, we used turbidostats[28] (**Supplementary Fig. 4** online), which enables accurate and automatic on-line measurements of population growth rates.

To quantify the relationship between population diversity and growth rate, we measured the growth rate dynamics as the population transitioned from one environment to the other. We first prepared separate cultures of fast and slow switchers by allowing them to reach a steady-state YFP expression distribution in environment E_1 or E_2 (**Fig. 2a**,**b**, bottom panels). Subsequently, we transferred cells to the other environment (at time $t = 0$) and monitored the population growth rate γ (**Fig. 2c**,**d**). When the environment was switched from E_2 to E_1, the growth rate of both the fast and slow switchers initially decreased rapidly within the first few hours, as most cells were initially in the unfit (OFF) state and were unable to produce their own uracil (**Fig. 2c**). After a lag period of 3–5 h, both fast- and slow-switching populations began to increase their growth rates, and they reached a steady-state growth rate after about 18 h (**Fig. 2c** and **Supplementary Fig. 5** online).

Although the growth rates for fast and slow switchers showed qualitatively similar dynamics, the quantitative differences between them illustrate the effects of diversity on the transient and steady-state growth rates. First, the fast switchers reached their steady-state about 4 h sooner than the slow switchers. This is because they enter the new environment with a larger population of fit (ON) cells, and also because more members of the initially large fraction of unfit (OFF) cells can switch to the fit (ON) state during the first few hours. During this initial phase, the fast-switching strategy is more competitive than the slow-switching strategy. However, once the growth rates have

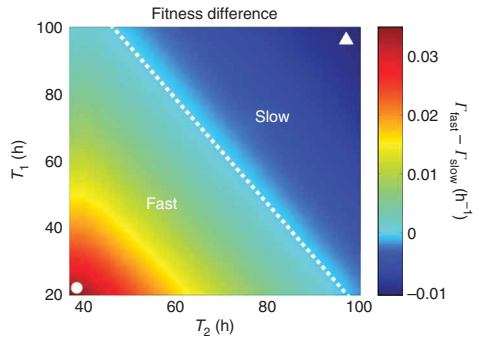

Figure 3 Model predictions for fluctuating environments. Heat map showing the predicted fitness difference (mean growth rate) between fast and slow-switching cells as a function of the environmental period (T_1, T_2). For short periods, the fast switchers show higher mean growth rates. On the other hand, for longer periods, slow switchers show a fitness advantage over the fast switchers. The dashed line separates regions where fast or slow switchers are predicted to be more fit. Two points were chosen in each part of the phase diagram to be further explored. The values of these points correspond to $T_1 = 20$ h, $T_2 = 37$ h (circle) and $T_1 = 96$ h, $T_2 = 96$ h (triangle).

reached steady state, the slow-switching strategy becomes more competitive, because the slow switchers transition less frequently to the unfit (OFF) phenotype. This results in a systematically larger steady-state growth rate compared to the fast-switching strategy. We observed similar growth rate dynamics when cells transitioned from E_1 to E_2 (**Fig. 2d**). The transient dynamics were slower overall in E_2, most probably because of a slow synthesis of the toxic intermediate 5-fluorouracil. In E_2, the slower recovery time and greater overlap between the fast and slow growth curves made it difficult to resolve the timing of recovery with as great a precision as was possible in E_1, and measurements of the relative timing of adaptation between fast and slow-switching populations were less accurate. After the adaptation period in E_2, both fast and slow switchers showed similar growth rates to what was observed in environment E_1 (**Fig. 2c**). Taken together, these results show that after transitioning to a new environment, fast switchers have higher growth rates than the slow switchers during the transition to steady state, but lower growth rates during the steady state itself.

To further demonstrate that the observed behavior was due to the differences in switching rates between fast and slow switchers, we built a quantitative model composed of ordinary differential equations. The model (see Methods) quantifies the number of cells in each of the two discrete phenotypes, ON and OFF, which confer different growth rates: $\gamma_{ON}(t)$ and $\gamma_{OFF}(t)$, respectively (**Fig. 1a**).These growth rates reflect the fitness advantage or disadvantage conferred by the surrounding medium by quantifying both the steady-state growth rate of each phenotype as well as the time required for each phenotype to reach steady state (**Supplementary Fig. 6** online). In addition, cells also transition from the OFF to ON (or ON to OFF) phenotypes at a constant rate r_{ON} (r_{OFF}), as shown in **Figure 1a**. The model was then fit to the experimental data taken in each environment (red and blue lines, **Fig. 2c,d**). The only differences between fast and slow-switching cells in the model are the transition rates (r_{ON}, r_{OFF}), indicating that the observed differences between fast and slow-switching cells can be accounted for by switching rates alone.

Using this population dynamics model, we can now predict which of the two switching strategies is more beneficial in fluctuating environments. In the model, the environment periodically alternates between environment E_1 (with a duration T_1) and E_2 (with a duration T_2) (**Fig. 1a**). To compare the relative advantage of one strategy over the other, we defined Γ to be the average population growth rate over one period and calculated the resulting growth rates as a function of T_1 and T_2 for the fast (Γ_{fast}) and slow (Γ_{slow}) switching strategies. For both strategies, rapidly fluctuating environments lead to decreased fitness levels, as more time is spent in the transient recovery stage of growth. However, the fitness difference between slow switching and fast-switching populations can either be positive or negative depending on T_1 and T_2 (**Fig. 3**). This analysis predicts that in rapidly changing environments, fast switchers would out-compete the slow switchers, whereas in slowly varying environments, the slow switchers would dominate. The dashed line in **Figure 3** shows which of the two strategies is more beneficial given the times T_1 and T_2.

To experimentally test these predictions, we chose two points in the (T_1, T_2) space to measure fitness: $T_1 = 20$ h, $T_2 = 37$ h (circle, **Fig. 3**) and $T_1 = 96$ h, $T_2 = 96$ h (triangle, **Fig. 3**). As with the previous experiments, we grew the cells to steady state (4 d) in E_2, and then transitioned them to E_1 at $t = 0$. After T_1 hours, the extracellular environment was changed again to E_2 for an additional T_2 hours (**Fig. 4**). The dynamically measured growth rates for these two fluctuating environments are shown for both fast and slow-switching populations (**Figs. 4a,b**), along with the population growth rates predicted by the model (solid lines). As the phase diagram suggests,

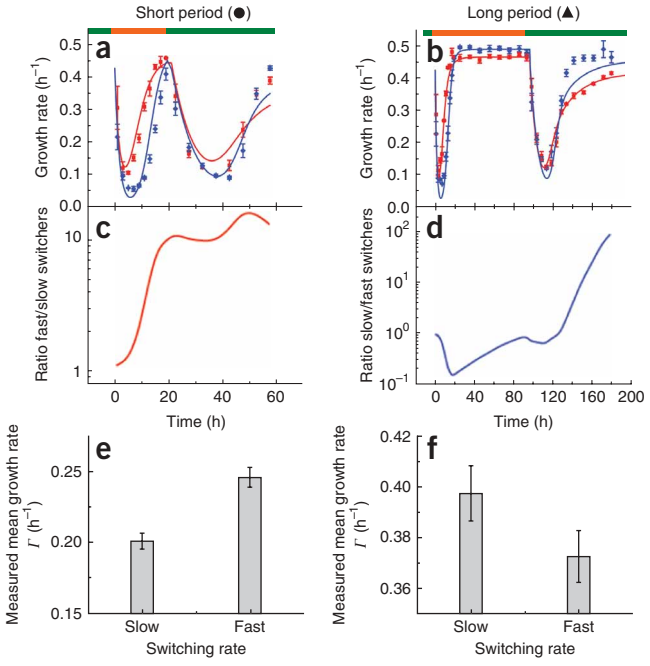

Figure 4 Testing the model predictions: growth dynamics in fluctuating environments with short and long periods. (**a**,**b**) Measured growth rates for fast (red) and slow (blue) switchers grown in the short-period environment (**a**) (20 h in E_1, 37 h in E_2, circle in **Fig. 3**) and the long-period environment (**b**) (96 h in E_1, 96 h in E_2, triangle in **Fig. 3**) are compared to the growth rates predicted by the model (solid lines). (**c**) The calculated ratio of the number of fast switchers to slow switchers in the short-period environment. (**d**) The calculated ratio of the number of slow switchers to fast switchers in the long-period environment. (**e**,**f**) The experimentally measured mean growth rate in the short period (**e**) and the long period (**f**) environments. Error bars represent a 2.8% error estimated from the s.d. of the growth rate measurements.

the fast-switching cells out-compete the slow switchers in the rapidly changing environment (**Fig. 4a**), whereas the situation is reversed in the slowly changing environment (**Fig. 4b**). The fitness difference between the fast and slow switchers as quantified by the average growth rate (**Fig. 4e**,**f**) shows that in the rapidly changing environment, the difference between growth rates is 20%, whereas in the slowly changing environment, it is 6%. Because of exponential population growth, these differences considerably magnify the relative competitiveness over even moderate timescales. This out-competition is made dramatically obvious when comparing the relative number of fast to slow switchers that would have been produced in a nonlimiting environment at the end of each run (**Fig. 4c**,**d**).

Our data suggest that tuning phenotypic switching rates may constitute a simple strategy to cope with fluctuating environments. Following this strategy, an isogenic population would improve its fitness by optimizing phenotypic diversity so that, at any given time, an optimal fraction of the population is prepared for an unforeseen environmental fluctuation. The diversity is introduced naturally through the stochastic nature of gene expression, allowing isogenic populations to mitigate the risk by 'not putting all of their eggs in one basket'. Recent work suggests that in an adverse environment, cell-to-cell variability can have an impact on the fitness of a population[29,30]. Here we show that, in fluctuating environments, it is the frequency of the environmental fluctuations that constrains the inter-phenotype transition rates. In particular, we demonstrate a possible mechanism for a population to enhance its fitness in fluctuating environments by tuning the phenotypic switching rates with respect to the duration of exposures to alternating environments. This 'resonant' condition provides an effective survival strategy by 'blindly' anticipating environmental changes. This strategy could be used by cellular populations that lack dedicated signal transduction machinery for particular extracellular signals, or when it is crucial for a population to act at a faster timescale than is possible by signal transduction.

METHODS

Strain construction. In order to couple the expression of the *URA3* gene to the activity of the galactose pathway, we modified the diploid strain MA0188 (ref. 24). The promoter of the *URA3* gene was replaced by the *GAL1* promoter using homologous recombination of transformed PCR product. The *Candida albicans HIS5* gene was used as a marker. Integrations were verified by PCR.

Growth conditions and media. We grew cultures in synthetic dropout media with the appropriate amino-acid supplement and 2% raffinose as a carbon source. Before transferring them to their turbidostat environments, we grew cells for 4 d in liquid culture in a shaker at 30 °C. The culture volume was 5 ml for the initial overnight growth and 10–15 ml afterwards. These 'pre-turbidostat' media (corresponding to environment E_2) contained uracil (at a final concentration of 0.02 mg/ml) and 5-FOA (at a final concentration of 0.19 μg/ml). During this period, cells were prevented from reaching stationary growth phase by serial dilution. Next, cells were washed with their prospective 'in-turbidostat' media (environment E_1 lacking uracil and 5-FOA) and transferred to the turbidostat. The turbidostat maintains constant optical density levels (OD) corresponding to exponential growth ($0.05 < OD_{600} < 0.2$). For the switch to environment E_2, we added uracil (0.02 mg/ml) and 5-FOA (0.19 μg/ml) to the turbidostat media. The turbidostat temperature was maintained at 30 °C. Fast and slow-switching phenotypes were obtained by supplementing the synthetic dropout media with galactose and doxycycline. For the fast-switching phenotype, we used 0.004% galactose and 0.00282 μg/ml doxycycline; for the slow-switching phenotype, we used 0.03% galactose and 0.0135 μg/ml doxycycline. The expression distributions were determined by flow cytometer (FACScan; Becton Dickinson).

The top panels in **Figure 2** show the distribution of the cells when they were grown in nonselective media conditions (with uracil and without 5-FOA) for 4 d after an overnight growth in nonselective media again). The fast and slow switchers have indistinguishable growth rates in nonselective media (**Supplementary Methods** online).

Measurement of switching rates. Cells were grown using nonselective synthetic dropout media (including 0.02 mg/ml uracil but lacking 5-FOA) in 2% raffinose. After overnight growth, cells were grown in 5-ml cultures for 30 h in 2% raffinose ('raffinose history') and 2% raffinose and 2% galactose ('galactose history'). Subsequently, the raffinose and galactose history cells were separately grown for another 24 h in media having 0.004% galactose and 0.00282 μg/ml doxycycline (fast switchers) and 0.03% galactose and 0.0135 μg/ml doxycycline (slow switchers). Culture volume during this period was 10 ml, and the OD did not exceed 0.315. The expression distributions shown in **Supplementary Figure 1** were determined by flow cytometer (FACScan; Becton Dickinson).

We used a first-order kinetic model to estimate the amount of time required for a cell to transition from one state to the other once it has decided to make the switch. Here we assumed that ON cells produce YFP and Ura3 protein at a constant rate and that OFF cells produce none. Further, we assumed that removal of YFP and Ura3 was determined by the dilution rate due to growth. Using this model, we calculated that it requires approximately 1.3 h for an average OFF cell to enter into the ON phenotype peak, whereas it requires approximately 6.5 h for an ON cell to dilute enough YFP to be indistinguishable from an OFF cell. Both of these timescales are smaller that the switching rates, indicating that our approximation of the population as two distinct phenotypes is reasonable.

Turbidostat setup. All growth rate measurements were made using a custom-made turbidostat (**Supplementary Fig. 4**). Cells were maintained at 10–15 ml volumes in test tubes while magnetic stir bars kept the cultures well mixed. An infrared LED/Photodiode pair (940 nm) was used to measure the relative OD through a D/A converter and custom Labview software. A peristaltic pump provided fresh media to dilute the population whenever the OD went above a critical threshold value. A second continuously operating peristaltic pump coupled to a pickup tube kept the culture volume fixed.

Population dynamics model. The model consists of two differential equations that characterize the dynamics of the number of cells in the ON and OFF states, N_{ON} and N_{OFF}, respectively:

$$(d/dt)N_{ON} = \gamma_{ON}N_{ON} - r_{OFF}N_{ON} + r_{ON}N_{OFF}$$
$$(d/dt)N_{OFF} = \gamma_{OFF}N_{OFF} + r_{OFF}N_{ON} - r_{ON}N_{OFF}$$

The population growth rate is given by:

$$\gamma(t) = \frac{(d/dt)N_{ON} + (d/dt)N_{OFF}}{N_{ON} + N_{OFF}}$$

The parameter r_{ON} (r_{OFF}) characterizes the rate of transitions to the ON (OFF) state. The values γ_{ON} and γ_{OFF} are the instantaneous growth rates of the ON and OFF phenotypes and depend on which environment the cells are in. In E_1 the rates are given by $\gamma_{ON}(t) = \gamma_1(1 - e^{-r_1 t})$ and $\gamma_{OFF}(t) = \gamma_1(e^{-d_1 t})$, and in E_2 the rates are given by $\gamma_{OFF}(t) = \gamma_2(1 - e^{-r_2 t})$ and $\gamma_{ON}(t) = \gamma_2(e^{-d_2 t})$ (**Supplementary Fig. 6**). In these equations, t represents the amount of time since the last environmental transition, and the constants γ_1 and γ_2 represent the steady-state growth rates achieved by the fit phenotype in each environment. The constants r_1 and r_2 represent the amount of time it takes cells to recover from a transition from an unfit to a fit environment. Similarly, d_1 and d_2 represent the time it takes unfit cells to cease growing after a transition from a fit environment to an unfit environment. Parameters and their values are detailed in **Supplementary Table 1** online. The model results were calculated using the ode23 function in Matlab (Mathworks). We fit the parameters r_1, r_2, d_1 and d_2 to the data in **Figure 2c** and **d** by minimizing the χ^2 cost function with custom Matlab scripts.

Data analysis. We calculated growth rates by recording the fraction of time the pump was actively providing fresh media during each hour-long interval and converting this into a pump flow rate by multiplying by the pump's maximal possible flow rate. This raw pump activity was then converted into a growth rate by normalizing with the volume of the turbidostat culture using the

formula $\gamma(t) = \frac{p(t)}{V_{\text{culture}}}$, where $p(t)$ represents the measured pumping rate in ml/hr and V_{culture} represents the culture volume in ml.

Note: Supplementary information is available on the Nature Genetics website.

ACKNOWLEDGMENTS

We would like to thank M. Thattai, S. Tans, A. Raj, J. Gore, S. Rifkin and N. Karahan for helpful discussions and/or comments on the manuscript. This work was supported by National Science Foundation grant PHY-0548484 and US National Institutes of Health grant R01-GM077183. J.T.M. was partially supported by an NSF Graduate Research Fellowship.

AUTHOR CONTRIBUTIONS

M.A. and A.v.O. conceived the project and designed the experiments. M.A. constructed and characterized the yeast strain used and performed the turbidostat experiments. J.T.M. built the turbidostat and developed the population dynamics model. All authors interpreted the results and wrote the paper.

Published online at http://www.nature.com/naturegenetics
Reprints and permissions information is available online at http://npg.nature.com/reprintsandpermissions

1. Cohen, D. Optimizing reproduction in a randomly varying environment. *J. Theor. Biol.* **12**, 119–129 (1966).
2. Levins, R. *Evolution in Changing Environments: some Theoretical Explorations* (Princeton University Press, Princeton, New Jersey, 1968).
3. Schaffer, W.M. Optimal efforts in fluctuating environments. *Am. Nat.* **108**, 783–790 (1974).
4. Stearns, S.C. Life-history tactics: a review of the ideas. *Q. Rev. Biol.* **51**, 3–47 (1976).
5. Paulsson, J. Summing up the noise in gene networks. *Nature* **427**, 415–418 (2004).
6. Kaern, M., Elston, T.C., Blake, W.J. & Collins, J.J. Stochasticity in gene expression: from theories to phenotypes. *Nat. Rev. Genet.* **6**, 451–464 (2005).
7. Samoilov, M.S., Price, G. & Arkin, A.P. From fluctuations to phenotypes: the physiology of noise. *Sci. STKE* **2006**, re17 (2006).
8. Kaufmann, B.B. & van Oudenaarden, A. Stochastic gene expression: from single molecules to the proteome. *Curr. Opin. Genet. Dev.* **17**, 107–112 (2007).
9. Maheshri, N. & O'Shea, E.K. Living with noisy genes: how cells function reliably with inherent variability in gene expression. *Annu. Rev. Biophys. Biomol. Struct.* **36**, 413–434 (2007).
10. Kussell, E., Kishony, R., Balaban, N.Q. & Leibler, S. Bacterial persistence: a model of survival in changing environments. *Genetics* **169**, 1807–1814 (2005).
11. Kussell, E. & Leibler, S. Phenotypic diversity, population growth, and information in fluctuating environments. *Science* **309**, 2075–2078 (2005).
12. Lachmann, M. & Jablonka, E. The inheritance of phenotypes: an adaptation to fluctuating environments. *J. Theor. Biol.* **181**, 1–9 (1996).
13. Thattai, M. & van Oudenaarden, A. Stochastic gene expression in fluctuating environments. *Genetics* **167**, 523–530 (2004).
14. Wolf, D.M., Vazirani, V.V. & Arkin, A.P. Diversity in times of adversity: probabilistic strategies in microbial survival games. *J. Theor. Biol.* **234**, 227–253 (2005).
15. Dubnau, D. & Losick, R. Bistability in bacteria. *Mol. Microbiol.* **61**, 564–572 (2006).
16. Avery, S.V. Microbial cell individuality and the underlying sources of heterogeneity. *Nat. Rev. Microbiol.* **4**, 577–587 (2006).
17. Casadesus, J. & Low, D. Epigenetic gene regulation in the bacterial world. *Microbiol. Mol. Biol. Rev.* **70**, 830–856 (2006).
18. Hasty, J., Pradines, J., Dolnik, M. & Collins, J.J. Noise-based switches and amplifiers for gene expression. *Proc. Natl. Acad. Sci. USA* **97**, 2075–2080 (2000).
19. Kepler, T.B. & Elston, T.C. Stochasticity in transcriptional regulation: origins, consequences, and mathematical representations. *Biophys. J.* **81**, 3116–3136 (2001).
20. Atkinson, M.R., Savageau, M.A., Myers, J.T. & Ninfa, A.J. Development of genetic circuitry exhibiting toggle switch or oscillatory behavior in *Escherichia coli*. *Cell* **113**, 597–607 (2003).
21. Becskei, A., Seraphin, B. & Serrano, L. Positive feedback in eukaryotic gene networks: cell differentiation by graded to binary response conversion. *EMBO J.* **20**, 2528–2535 (2001).
22. Gardner, T.S., Cantor, C.R. & Collins, J.J. Construction of a genetic toggle switch in *Escherichia coli*. *Nature* **403**, 339–342 (2000).
23. Isaacs, F.J., Hasty, J., Cantor, C.R. & Collins, J.J. Prediction and measurement of an autoregulatory genetic module. *Proc. Natl. Acad. Sci. USA* **100**, 7714–7719 (2003).
24. Acar, M., Becskei, A. & van Oudenaarden, A. Enhancement of cellular memory by reducing stochastic transitions. *Nature* **435**, 228–232 (2005).
25. Smits, W.K., Kuipers, O.P. & Veening, J.W. Phenotypic variation in bacteria: the role of feedback regulation. *Nat. Rev. Microbiol.* **4**, 259–271 (2006).
26. Hawkins, K.M. & Smolke, C.D. The regulatory roles of the galactose permease and kinase in the induction response of the GAL network in *Saccharomyces cerevisiae*. *J. Biol. Chem.* **281**, 13485–13492 (2006).
27. Boeke, J.D., LaCroute, F. & Fink, G.R. A positive selection for mutants lacking orotidine-5′-phosphate decarboxylase activity in yeast: 5-fluoro-orotic acid resistance. *Mol. Gen. Genet.* **197**, 345–346 (1984).
28. Bryson, V. & Szybalski, W. Microbial selection. *Science* **115**, 45–51 (1952).
29. Blake, W.J. *et al.* Phenotypic consequences of promoter-mediated transcriptional noise. *Mol. Cell* **24**, 853–865 (2006).
30. Bishop, A.L., Rab, F.A., Sumner, E.R. & Avery, S.V. Phenotypic heterogeneity can enhance rare-cell survival in 'stress-sensitive' yeast populations. *Mol. Microbiol.* **63**, 507–520 (2007).